Compactness and Bracing Recommendations for Equal Leg Single Angle Beams

CHRISTOPHER J. EARLS

INTRODUCTION

Currently, the design of single angle members is governed by the *Load and Resistance Factor Design Specification for Single Angle Members* (AISC, 2000). The provisions in this document are meant to augment the more general design provisions contained in the *Load and Resistance Factor Design Specification for Structural Steel Buildings* (AISC, 1999). The design provisions contained in the *LRFD Specification for Design of Single Angle Members* are the result of the best information available at the time of the preparation of the document in the early, to mid, 1990s. In the intervening years, new information about single angle flexural response has accumulated from research efforts aimed at quantifying structural ductility associated with equal leg single angle beams. This new information will be summarized herein and recommendations made for rational enhancements to the *LRFD Specification for Design of Single Angle Members*.

CURRENT PRACTICE

The current *Load and Resistance Factor Design Specification for Single Angle Members* (AISC, 2000), hereafter referred to as the *Specification*, focuses on the five most common flexural orientations of the angle cross-section as encountered in practice. These orientations are displayed in Figure 1 in conjunction with the naming convention adopted in the present work. The subject orientations consist of both senses of minor principal and geometric axis flexure as well as major principal axis flexure. The current *Specification* (AISC, 2000) addresses both equal and unequal leg angles. The *Specification* views the case of equal leg single angle cross-sections as being a special case of the more general unequal leg scenario. However, since flexural applications (not involving continuous lateral bracing) most often involve equal leg angles, the present study focuses on equal leg angles only.

The three general flexural limit states considered in the *Specification* are: 1) local buckling when the tip of an angle leg is in compression; 2) yielding when the tip of an angle leg is in tension; and 3) lateral-torsional buckling of the angle beam.

In consideration of the first limit state, which is related to the local buckling of the compressed element of the angle cross-section, the *Specification* adopts limiting plate slenderness criteria that are based on the case of an unstiffened plate element subjected to uniform compression. This approach is thought to be conservative since the actual stress distribution in an angle beam will vary linearly through the beam depth and as such represents a less critical loading configuration of the angle cross-sectional plate component. Similarly, the slender element capacity reduction strategy adopted for angle beams in the *Specification* is simply that which is specified for use with angle columns composed of slender plate elements subjected to a uniform stress condition. Implied in this approach, here again, is that it is conservative to apply provisions formulated for use with column sections to the less critical stress distribution developed in flexural cross-sections. In any event, even if a particular angle cross-section satisfies the most stringent of the plate slenderness requirements, as outlined in the *Specification*, it is currently not permitted to rely on the development of the full plastic capacity of the cross-section in design calculations for cases of geometric axis flexure. Instead, the current *Specification* restricts the maximum single angle cross sectional capacity to be 1.5 times the yield moment, M_y: a value that can be much less than the plastic capacity of single angle cross-sections bent bout the geometric axis.

Originally, a cross sectional capacity limit of 1.25 times M_y was imposed in the earlier version of the *Load and Resistance Factor Design Specification for Single Angle*
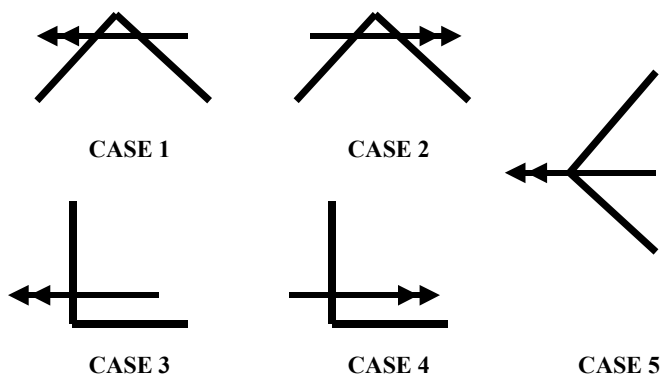
Fig. 1. Common single angle flexural orientations.

Christopher J. Earls is assistant professor and William Kepler Whiteford Faculty Fellow, department of civil and environmental engineering, University of Pittsburgh, Pittsburgh, PA.

Members (AISC, 2000) due to concerns that single angles were incapable of developing their full-plastic capacity (in addition to the fact that it was thought large cross-sectional distortions might exist at the high stress levels needed to attain M_p). These concerns have been alleviated as a result of the analytical and experimental studies carried out in recent years (Earls and Galambos, 1997a; Madugula, Kojima, Kajita, and Ohama, 1995, 1996). As a result of this work, the current *Load and Resistance Factor Design Specification for Single Angle Members* (AISC, 2000) has raised the limit on the maximum cross sectional moment capacity for single angles to be 1.5 times M_y. While this is an improvement, it will be shown that further increases in single angle cross-sectional capacity are justified.

The single angle flexural capacity limitation just discussed, impacts directly on the second general flexural limit state addressed in the *Specification* and relating to the situation in which angle toes experience tension. The *Specification* recognizes that in this situation, local buckling effects are of little importance and hence the cross-sectional capacity can be assumed to be limited by those concerns previously associated with an angle beam's ability to develop its full plastic capacity. Here too it will be demonstrated that the current limitation of $1.5(M_y)$ is overly conservative for the case of equal leg single angle geometric axis flexure.

At the heart of the *Specification's* lateral-torsional buckling limit state provisions for angle beams are the theoretical elastic buckling solutions developed by Thomas and Leigh (Thomas and Leigh, 1973 and 1970). These elastic solutions are modified by the *Specification* for use in the inelastic range through the application of a linear inelastic transition zone (as outlined in section 5.1.3 of the *Specification*.) Modifications to the elastic case are also given in this same section of the *Specification* such that a reduction of between 8 percent and 25 percent, of the theoretical solu-

$$R = \left(\frac{\Theta_2}{\Theta_1} \right) - 1$$

Fig. 2. Definition of rotation capacity.

tions provided by Thomas and Leigh (Thomas and Leigh, 1973, 1970), are used for design. It is further noted that for the case of unbraced geometric axis flexure, the calculation of the yield moment (as required by the provisions in section 5.1.3 of the *Specification*) must be carried out with a reduction factor of 0.8 applied to the cross sectional elastic section modulus to account for anticipated out-of-plane deflections and twisting of the angle cross section due to the nature of non-principal axis flexure, and its resulting increase in compressive stresses in the toe of the angle beam. It will be shown in this paper that this limitation on the elastic section modulus is not required in a practical sense.

In addressing the inelastic flexural behavior of single angles it is often useful to employ plastic analysis and design methodologies. These techniques are philosophically consistent with modern limit states design specifications and are quite easy to apply, thus helping to simplify complicated design problems. However, in order to apply these techniques reliably it is necessary that sufficient plastic hinge rotation capacity be available at the member level so as to develop a collapse mechanism at the structural system level. The *LRFD Specification for Structural Steel Buildings* (AISC, 1999) requires that a member section exhibit a minimum plastic hinge rotation capacity of three if that member is to be considered compact and hence suitable for proportioning with plastic analysis and design techniques. It is assumed by AISC that localized buckling effects may be de-coupled from more globalized buckling behavior and hence all compactness criteria are given solely in terms of a limiting width-to-thickness ratio, λ_p, for the associated plate elements of the cross-section under consideration. The values for these compactness parameters are prescribed in Table B5.1 of the *LRFD Specification for Structural Steel Buildings* (AISC, 1999) on a case-by-case basis. Absent from this table however is any reference to single angle flexure. The present paper hopes to provide needed information to the profession that will allow for the proportioning of angle beams using plastic analysis and design methodologies.

In any discussion of flexural ductility measured by rotation capacity it is important to give a precise definition of what is meant by this quantity. The current paper adopts the definition for rotation capacity given by the American Society of Civil Engineers (ASCE, 1971), in which $R = \{(\theta_u/\theta_p) -1\}$ where θ_u is the rotation when the moment capacity drops below M_p on the unloading branch of the moment-rotation plot and θ_p is the rotation at which the full plastic capacity is first achieved assuming a perfectly elastic response. This definition is graphically presented in Figure 2 in which θ_1 corresponds to θ_p and θ_2 corresponds to θ_u.

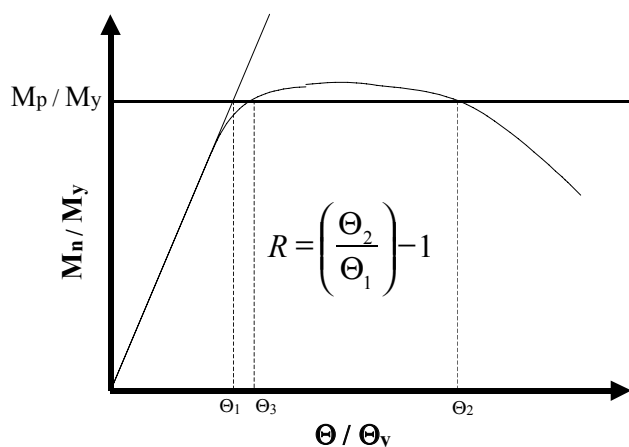The previously mentioned definition of flexural ductility is employed in characterizing results obtained from nonlin-

ear finite element studies of equal leg single angle beams. The nonlinear finite element method is the technique upon which all the conclusions of this paper are based. Since this is the case, a detailed description of the experimentally verified modeling techniques will be presented.

The present paper summarizes equal leg single angle compactness criteria suitable for use with plastic analysis and design methodologies. Hot-rolled angles made from steel having a yield strength less than or equal to 552 MPa (and also exhibiting a yield plateau prior to strain hardening during a uniaxial tension test) are considered. Such a steel is assumed to have an F_u / F_y ratio of approximately 1.5 as well as $\varepsilon_u / \varepsilon_y = 45$ and $\varepsilon_{st} / \varepsilon_y = 5.5$ and thus may be considered as a type of mild carbon steel (although it is recognized that current mild carbon steels cannot achieve such high yield strengths).

NONLINEAR FINITE ELEMENT MODELING

The commercial multipurpose finite element software package ABAQUS (ABAQUS, 1999) is employed in this research. Since the research reported herein spans a five year period, various versions of ABAQUS starting with version 4.8 up to the current 5.8-14 have been employed at one time or another. Irrespective of the version, ABAQUS has always had the ability to consider both geometric and material nonlinearity in a given model. Advantage has been taken of this capability and thus all modeling herein considers both nonlinear geometric and material influences. Incremental solution strategies are required to trace the proper nonlinear equilibrium path in analyses such as these; hence the modified Riks-Wempner solution strategy (ABAQUS, 1999; Riks, 1972 and 1979; Crisfield, 1981) is chosen for this work. In the earlier phases of the reported research work, it was thought to be important that residual stresses be adequately modeled in the angle cross-section. To this end, the residual stresses associated with hot rolling of the angle member were incorporated into the early finite element models by way of the ABAQUS user subroutine feature. In this way, residual stresses were imposed on the model by assigning initial stress values at the Gauss points of the shell elements prior to the first equilibrium iteration. The initial stresses assigned to the Gauss points were based on the residual stress patterns found in the literature (Usami and Galambos, 1971; Madugula and Kennedy, 1985). It was later found that influence of residual stresses on the structural ductility of hot-rolled angle beams was insignificant (Earls 1999b) and these stresses are not modeled in the more recent studies.

A similar situation arises in the case of initial imperfections superimposed on the perfect finite element mesh for the purposes of performing stability analyses. In general, for modeling studies where inelastic buckling is being stud-

ied it is important that the evolution of the modeling solution be carefully monitored so that any indication of bifurcation in the equilibrium path is carefully assessed so as to guarantee that the equilibrium branch being followed corresponds to the lowest energy state of the system (i.e. the configuration that nature will follow in the physical world). While different strategies exist for guaranteeing that the lowest energy path is taken (Teh and Clarke, 1999), the strategy of seeding the finite element mesh with an initial displacement field (ABAQUS, 1999) is employed in the later studies making up the body of knowledge related to single angle compactness discussed herein. In such a technique, the finite element mesh is subjected to a linearized-eigenvalue buckling analysis from which an approximation to the first buckling mode of the angle is obtained. The displacement field associated with this lowest mode is then superimposed on the finite element model as a seed imperfection for use in the incremental nonlinear analysis. This seed imperfection displacement field is scaled so that the maximum initial displacement anywhere in the mesh is equal to one-one-thousandth of the maximum unbraced length of the angle ($L_b / 1000$). While it is recognized that the technique of seeding a finite element mesh with an initial imperfection has shortcomings (Teh and Clarke, 1999), this technique is nonetheless employed in the current study due to the fact that results obtained from this method have agreed quite well with experimental tests obtained from the single angle literature. In addition, experience in modeling related problems has shown that neglect of imperfection seeding in the mesh does not result in significantly different modeling results in most cases involving hot-rolled single angle flexural members (Earls, 1995). As a result of this fact, much of the earlier compactness work was carried out on meshes that had no intentional imperfection imposed on them. However, very good results were nonetheless achieved (including early experimental verification studies). This is partially due to the fact that in many cases considered, initial loading of the mesh caused early deflections of the structure which effectively eliminated the possibility of a bifurcation in the primary equilibrium path (and its resulting numerical challenges). It is further noted that very small but finite imperfections exist in the mesh, unintentionally, due to the finite precision associated with the floating-point mathematics of the computing platforms used.

Finite Element Mesh

The models of the single angle beams considered in this study are constructed from a dense mesh of nine node shell finite elements. The planes of the mesh surfaces correspond with the middle surfaces of the constituent single angle cross-sectional plate components (see Figure 3). The mesh density used throughout this work was arrived at from

a mesh convergence study carried out as part of an earlier study (Earls, 1995). A constant moment loading is used in this work since it represents the most severe flexural condition for the single angle beams and has been the basis for steel beam design provisions of the past. Design provisions based on such constant moment loading scenarios can be extended to other, less critical, loading cases through the use of moment-gradient amplification factors such as that obtained with the C_b equation included in Chapter F of the *LRFD Specification for Structural Steel Buildings* (AISC, 1999). It is, however, mentioned that the *Specification* limits the value of C_b to be less than or equal to 1.5 for single angle beams.

The constant moment loading considered in the present work is achieved by applying concentrated forces perpendicular to the beam longitudinal axis at two points on a simply supported span as depicted in Figure 4. The concentrated forces are applied to the single angle shear center so as not to induce a primary torsional loading of the beams. Both end segments of the model experience a less critical moment gradient loading and are not studied in this research. Since these end segments are not considered, they are modeled as being approximately rigid through the use of an exaggerated shell thickness and by restricting the end segment material response to be purely elastic. In addition, the elastic modulus in both end segments is defined to be two orders of magnitude greater than the actual modulus of

elasticity used for steel within the central test section. In this central region of the beam, high mesh densities are used in order that phenomena such as localized buckling may be allowed to develop in the model. In the end segments however, such high mesh density is unwarranted and thus larger elements are used in these regions in the interest of computational efficiency. Inter-element compatibility within the graded mesh is ensured at the mesh transition interfaces through the use of the ABAQUS Multi-Point Constraint feature (ABAQUS, 1999). Restraint against out-of-plane translation is enforced for all nodes at the interface between the rigid and flexible regions of the beam. Similarly, twisting and warping of the single angle cross-section are constrained at the rigid-flexible transition interface as well.

The ABAQUS S9R5 nonlinear shell finite element is used for all modeling reported here. The S9R5 shell element is shear deformable and subsequently both reduced integration and discrete Kirchoff theory are employed to improve the overall thin-shell behavior of the S9R5 element: a 2x2 Gauss quadrature is used in-plane and the discrete Kirchoff condition is imposed at a finite number of points on the shell reference surface by way of a penalty function (ABAQUS, 1999). The transverse shear strains of the S9R5 are measured as the changes in the projections of the shell normal, at a point on the Gaussian shell reference surface, to tangents to the shell reference surface. It should be noted that these transverse shears are always treated elas-
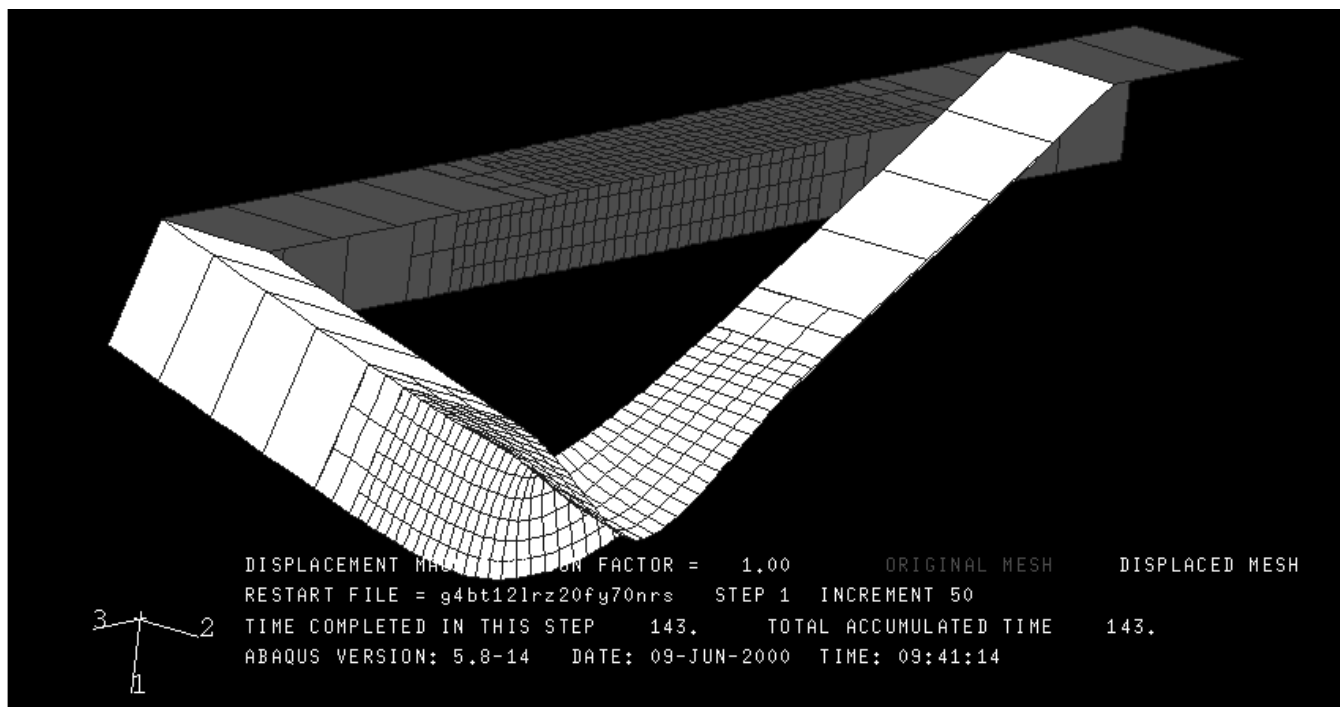

Fig. 3. Representative finite element mesh.

tically. The through-thickness integration is accomplished with Simpson's rule of fifth order.

In general, the S9R5 formulation is considered to be a large displacement, small strain type formulation. Despite the fact that this element is formulated for small strain applications, it nonetheless performs quite well in applications requiring the correct modeling of moderate to large strain behavior as evidenced from experimental verifications associated with similar problems to those treated herein (Earls, 2000; Earls and Galambos, 1997a).

A uniaxial representation of the constitutive law employed in this study appears in Figure 5 as a plot of true stress versus logarithmic strain. This piece-wise linear model has a yield stress that varies as a parameter of the study. Hence, the ratio F_u / F_y also varies within the study, but in all cases $\varepsilon_u / \varepsilon_y = 45$ and $\varepsilon_{st} / \varepsilon_y = 5.5$. ABAQUS uses the von Mises yield criterion to extrapolate a yield surface

in three-dimensional principal stress space based on the assumed uniaxial material response described above and in Figure 5. The corresponding ABAQUS metal plasticity model is characterized as being an associated flow plasticity model with isotropic hardening being used as the default.

Despite the sometimes very high yield strengths considered in the present study, mild carbon steel best describes the steel composition based on the yield plateau length and strain-hardening slope. Practically speaking however, it is recognized that mild carbon steel currently is incapable of achieving such high strengths. Five distinct yield strengths of steel are studied herein: 276 MPa, 345 MPa, 414 MPa, 483 MPa, and 552 MPa. The inelastic portion of the constitutive response is held constant over variations in yield strength. Thus, as a change in yield stress occurs, the plastic plateau and strain hardening regions simply slide up or
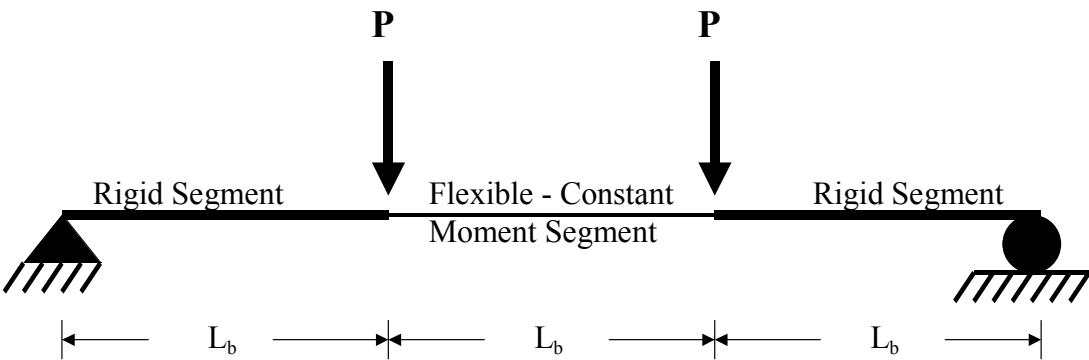

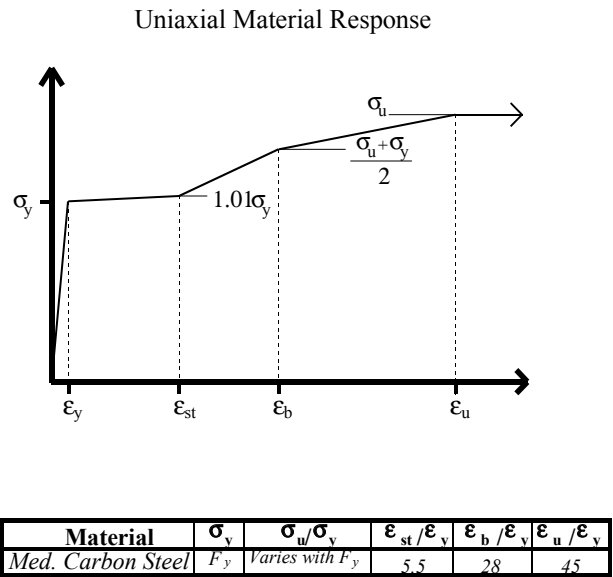Fig. 4. Schematic of overall specimen geometry and loading.

Uniaxial Material Response

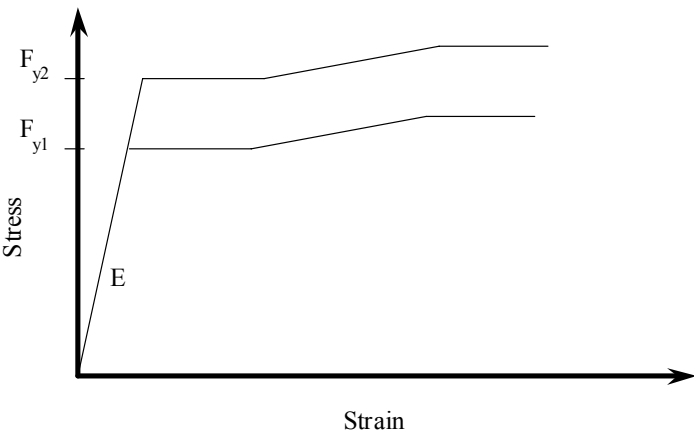| Material	σ_y	σ_u/σ_y	$\varepsilon_{st}/\varepsilon_y$	$\varepsilon_b/\varepsilon_y$	$\varepsilon_u/\varepsilon_y$
Med. Carbon Steel	F_y	Varies with F_y	5.5	28	45

Fig. 5. Uniaxial constitutive response used in models.

Fig. 6. Assumed inelastic behavior at various yield strengths.

Table 1. Summary of Case 1 Compactness Results														
F_y = 276 MPa			F_y = 345 MPa			F_y = 414 MPa			F_y = 483 MPa			F_y = 552 MPa		
b/t	L_b/r_z	R	b/t	L_b/r_z	R	b/t	L_b/r_z	R	b/t	L_b/r_z	R	b/t	L_b/r_z	R
6	280	3.2	6	200	3.1	6	160	3.2	6	140	3.1	6	115	3.2
8	145	3.2	8	110	3.1	8	93	3.1	8	79	3.1	8	66	3.1
10	101	3.1	10	74	3.1	10	55	3.0	10	38	3.2	10	30	3.1
12	51	3.5	12	36	3.3	12	25	3.3	12	20	3.9	12	18	3.1
14	25	3.9	14	15	3.1	14	11	3.3	14	8	3.0	14	7	3.0
16	14	3.1	16	7	3.0	16	5	5.1	16	5	3.3	16	4	5.3
18	6	3.4	18	5	3.8	18	4	5.2	18	4	3.9	18	3	6.3
20	5	3.2	20	4	4.3	20	3	7.6	20	3	5.1	20	3	4.1

down along a line whose slope is the initial material stiffness as shown in Figure 6.

Model Validation

Several validation studies have been carried out to demonstrate the usefulness and accuracy of the modeling techniques used to obtain the results presented herein (Earls and Galambos, 1997a; Earls, 2001a and 2001b). The verification studies involved comparisons to experimental tests conducted by Madugula et al. (Madugula et al., 1995 and 1996) and encompassed the flexural orientations of Cases 1 through 4. In general, a good agreement between the physical tests and the numerical modeling was achieved. Based on the favorable performance of the modeling techniques it has been concluded that they are experimentally verified and as such provide accurate and reliable results.

CASE 1. COMPACTNESS

In the case of minor principal axis flexure in which the angle toes are in compression (Case 1), varying only the yield stress of the mild carbon steel constitutive relationship, while maintaining all other material response parameters as constant, impacts profoundly on the plate slenderness parameter λ_p. In general it is noted that as the steel yield stress increases, the plate slenderness parameter decreases linearly as can be seen in the plot of Figure 7. This observed relationship is closely approximated by the predictive equation relating λ_p and F_y expressed below:

$$\lambda_p = 0.756\sqrt{\frac{E}{F_y}} - 1.67 \qquad (1)$$

Equation 1 is subject to the following limitations:
1. $6 \leq b/t \leq 20$
2. $276 \text{ MPa} \leq F_y \leq 552 \text{ MPa}$

Contrary to current design practice (AISC, 2000), in which it is assumed that the unbraced length of the single angle cross section has no impact on the Case 1 flexural response, some length dependence has been observed in recent research (Earls and Galambos, 1997b) focusing on this particular case. The mentioned research demonstrates that an increase in beam slenderness, L_b / r_z, of 132 percent only results in an overall decrease in rotation capacity of 26 percent. It is also noted that the observed relationship between rotation capacity and the beam unbraced length appears to be quadratic. Hence, the diminution of rotation capacity decreases as beam unbraced length increases. While this decrease in Case 1 single angle rotation capacity with increasing unbraced length is interesting, it is of little practical importance since overall angle deflections would almost certainly govern any realistic design employing plastic analysis and design techniques at beam lengths where such effects become important. Hence any practical discussion on single angle compactness for this case can safely ignore any length effects.
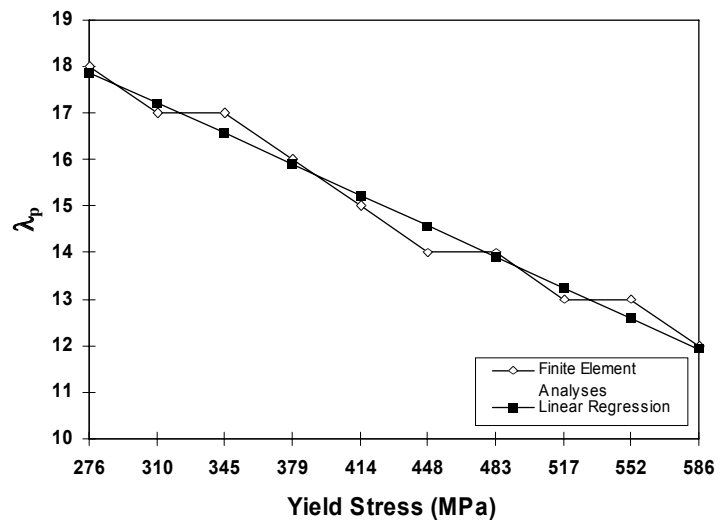

Fig. 7. Case 1 finite element compactness results.

CASE 2. COMPACTNESS

The minor principal axis flexural case in which the angle heel is in compression (Case 2) has been studied as part of recent research efforts (Earls and Galambos, 1997b and 1998). The Case 2 studies involve modeling the single angle cross-sections as being made from a number of possible steel grades ranging from mild carbon steel to very high strength quenched and tempered steels such as A514.

Based on these studies (Earls and Galambos, 1997b and 1998), it is noted that all hot-rolled steel angles currently manufactured in the United Sates are compact when subjected to Case 2 flexure. This statement is made realizing that increased steel yield strength reduces overall Case 2 rotation capacity, but further realizes that even for Case 2 single angles made from an unfavorable steel (from the standpoint of ductility) such as A514, compactness is still easily achieved with a single angle b/t ratio as high as 20.

CASE 3. COMPACTNESS

For the single angle geometric axis flexural case in which the horizontal leg is in tension, moment-rotation behavior is quite favorable in that adequate cross-sectional rotations can be obtained in a predictable manner prior to any excessive unloading due to localized buckling, global buckling, or combinations thereof. This favorable moment-rotation response is consistently obtainable with a careful control of plate slenderness (b/t) and beam slenderness (L_b / r_z) at a given steel grade.

λp for differing steel yield strengths

Legend:
- Fy=276MPa
- Fy=345MPa
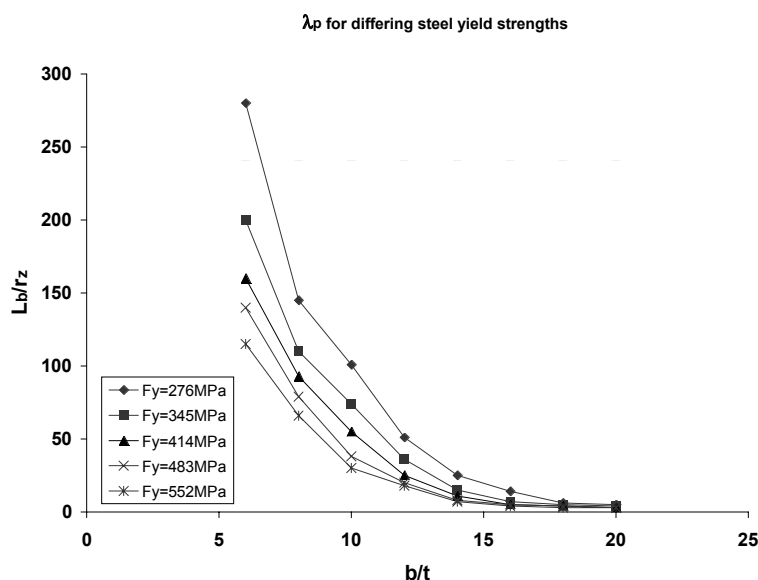- Fy=414MPa
- Fy=483MPa
- Fy=552MPa

Fig. 8. Case 3 finite element compactness results.

The results from the many finite element models carried out as part of the research into the behavior of this case are summarized in Table 1. In addition to this tabular format, a graphical presentation is made in Figure 8. It is mentioned that a definition of compactness, wherein the single angle beam, to be considered compact, must display a member rotation capacity, R, that falls within the range of 3.0 to 3.2, is adopted. However, as can be observed in Table 1, there are several cases in which the rotation capacity exhibited by some specimens far exceeds 3.0. This situation arises from the fact that plate slenderness values (b/t) are varied as integers and as a result, at high plate slenderness values occurring in angles made from steel with high yield strengths, a given b/t value can result in a rotation capacity of 1.5 while the next lower integer value might result in a rotation capacity of 5.0 for example. In these cases the integer plate slenderness yielding a rotation capacity that exceeds a value of 3.0 is selected as being associated with compactness. The use of integer values for the plate slenderness is adopted in the interest of expediency in such a large parametric study.

In Figure 8 a plot of beam slenderness versus plate slenderness is displayed for five different mild carbon steel yield strengths (276 MPa, 345 MPa, 414 MPa, 483 MPa, and 552 MPa). The trends exhibited by this plot are studied and the results from this study are presented in the following section.

It is apparent from Figure 8 that, at a given plate slenderness value, b/t, as the yield strength of the mild steel increases, the beam slenderness must diminish if compactness is to be maintained. In addition, for a given steel yield strength the relationship between beam slenderness, L_b / r_z, and the plate slenderness, b/t, is a nonlinear one. However, it can be observed in Figure 8 that in the range of plate slenderness from 18 to 20, all of the previously disparate response curves essentially merge into one. In addition, this single curve has a very linear character in this b/t range of 18 to 20. Based on curve fitting analyses in the range of yield strengths from 276 MPa to 552 MPa, where b/t ranges from 6 to 18, the response relationship between L_b / r_z and b/t appears to be cubic.

It is pointed out that the results contained herein are obtained from models that assume ideal restraint at the angle boundaries in terms of out-of-plane deflections, warping, and twisting. Normally field connection conditions do not qualify as being ideal and current design specifications (AISC, 1999) allow for the introduction of effective length factors for out-of-plane deflections, twisting, and warping (Galambos, 1968) in consideration of differing boundary conditions. However, while the application of effective length factors is entirely reasonable for design provisions based on rational modifications of classical elastic solutions, the present work may not lend itself to such an approach since the impact of the given set of boundary con-

ditions, while slight, appears to affect the inelastic mode shape in different ways on a case-by-case basis. Hence, any assumption of a uniform effective length factor appears to be inapplicable to this particular type of single angle geometric axis flexure.

The member response trends displayed in Figure 8 form the basis for the design methodology developed as part of the current research. This design method is described below.

Design Method

It is noted from Figure 8 that a design curve based on the L_b/r_z versus b/t behavior of the 552 MPa yield strength case could form a lower bound to the design space encompassing b/t values ranging inclusively from 6 to 20 for mild carbon steels possessing yield strengths less than or equal to 552 MPa. However, such an approach would be unduly

conservative especially for single angle beams with stocky cross sections that are rolled from lower strength steel.

As a result of numerical analyses of the data, an approach based on a weighted averaging of the bounding cases for steel whose strength is 276 and 552 MPa is adopted. The form of the following polynomial design equation (Equation 2) is the result of such an averaging of the bounding cases as discussed in earlier research (Earls, 2001a).

$$\frac{L_b}{r_z} = \frac{310.5}{F_y}\left\{-0.1258\left(\frac{b}{t}\right)^3 + 6.46\left(\frac{b}{t}\right)^2 - 111.72\left(\frac{b}{t}\right) + 658.89\right\}$$

(2)

Equation 2 is subject to the following limitations:
1. $6 \le b/t \le 20$
2. 276 MPa $\le F_y \le$ 552 MPa

The favorable agreement between this design equation and the finite element results can be observed in Figures 9 through 13.

It is noted that based on recent research (Earls, 2001c and 2001d), the requirement of the *Specification* that only 80 percent of the elastic section modulus be used in the case of unbraced geometric axis flexure seems to be unduly conservative. The *Specification's* imposed the 80 percent limit on the section modulus out of concern that out-of-plane deflections and twisting of the angle cross-section, due to the nature of non-principal axis flexure in this Case (and its resulting increase in compressive stresses in the toe of the angle beam), may adversely affect angle strength. This limit does not appear to be appropriate based on the results presented above.
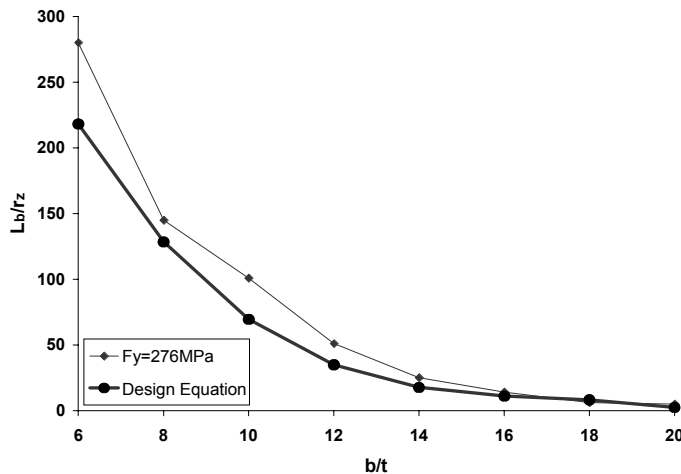

Fig. 9. Comparison of results between FEM and proposed Case 3 design equation.
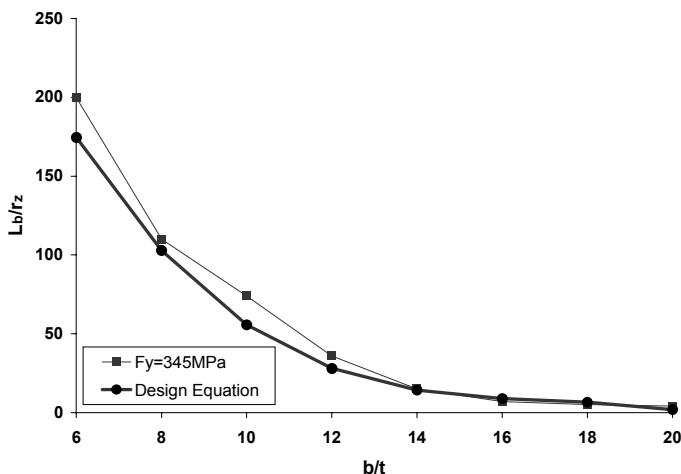

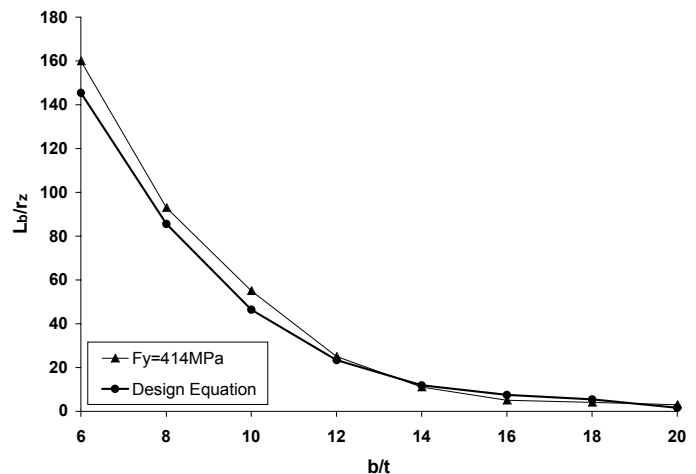Fig. 10. Comparison of results between FEM and proposed Case 3 design equation.

Fig. 11. Comparison of results between FEM and proposed Case 3 design equation.

Table 2. Summary of Case 2 Compactness Results														
F_y = 276 MPa			F_y = 345 MPa			F_y = 414 MPa			F_y = 483 MPa			F_y = 552 MPa		
b/t	L_b/r_z	θ_3/θ_1	b/t	L_b/r_z	θ_3/θ_1	b/t	L_b/r_z	θ_3/θ_1	b/t	L_b/r_z	θ_3/θ_1	b/t	L_b/r_z	θ_3/θ_1
6	400	1.74	6	260	1.65	6	220	1.72	6	190	1.65	6	165	1.65
8	185	1.67	8	130	1.68	8	120	1.75	8	100	1.66	8	90	1.68
10	90	1.65	10	65	1.65	10	60	1.69	10	50	1.66	10	45	1.67
12	50	1.75	12	30	1.67	12	26	1.65	12	20	1.69	12	25	1.65
14	28	1.71	14	20	1.67	14	15	1.69	14	12	1.66	14	15	1.72
16	10	1.74	16	10	1.69	16	10	1.71	16	10	1.73	16	10	1.74
18	6	1.74	18	6	1.75	18	6	1.75	18	6	1.73	18	6	1.74
20	5	1.75	20	4	1.68	20	4	1.67	20	4	1.71	20	4	1.67

CASE 4. COMPACTNESS

For Case 4 single angle geometric axis flexure, moment-rotation behavior is quite favorable in that very large cross-sectional rotations are easily obtained prior to any excessive unloading due to localized buckling, global buckling, or combinations thereof. A depiction of this type of characteristic moment-rotation behavior appears in Figure 14. In earlier research (Earls and Galambos, 1997a), compactness for this case of flexure was associated with the plate slenderness ratio (b/t) that resulted in the plateau of the moment-rotation response being coincident with the full cross-sectional capacity of an equal leg single angle member made from 345 MPa steel. In general however, this approach may not be practical since at higher yield stress the attainment of full cross-sectional plastic capacity could be delayed until relatively large cross-sectional rotations are reached (i.e. large values of θ_3 in Figure 2).

In order to address this issue a response measure of θ_3/θ_1 is defined (referring to the variables depicted in Figure 2). A representative value of approximately 1.3 for this ratio is identified as a reasonable approximation to the response of typical wide flanged flexural cross-sections based on exper-

imental results presented by Lay and Galambos (Lay and Galambos, 1965) as well as finite element modeling by Earls (Earls, 1999c). In the current case of single angle flexure however, it is quite common to achieve values well in excess of 1.3 if the earlier compactness criterion of Earls and Galambos (Earls and Galambos, 1997a) is used in conjunction with steel stronger than 345 MPa. It is surmised that if such large cross-sectional rotations are required in the attainment of full cross-sectional capacity in an angle beam then poor serviceability may arise from excessive deflections at modest overload states (somewhere between service load and ultimate load). It is also noted that at high yield stresses (i.e. higher than the 345 MPa considered by Earls and Galambos), the moment-rotation response may experience a significant increase in capacity over M_p prior to the manifestation of any plateau in response (see Figure 15). It is thus felt that a balance must be struck between controlling these early cross-sectional rotations and accounting for the significant strength reserve available in high strength steel single angles subjected to this type of flexure. As a result, a somewhat arbitrary increase of roughly 30 percent over the θ_3/θ_1 =1.3 of wide flange beams is considered to be a reasonable upper limit. Hence
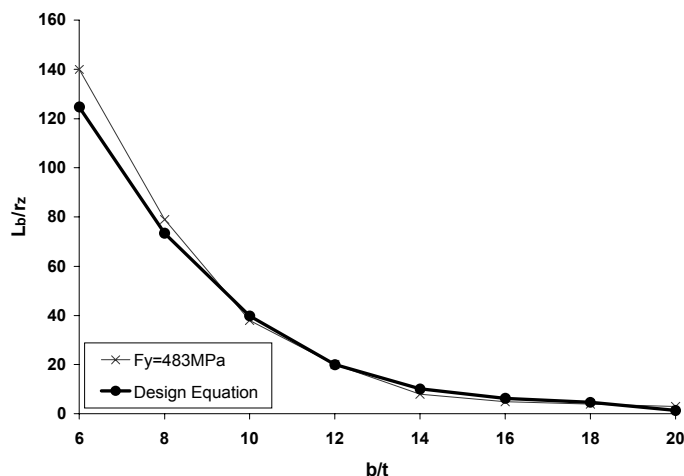
Fig. 12. Comparison of results between FEM and proposed Case 3 design equation.
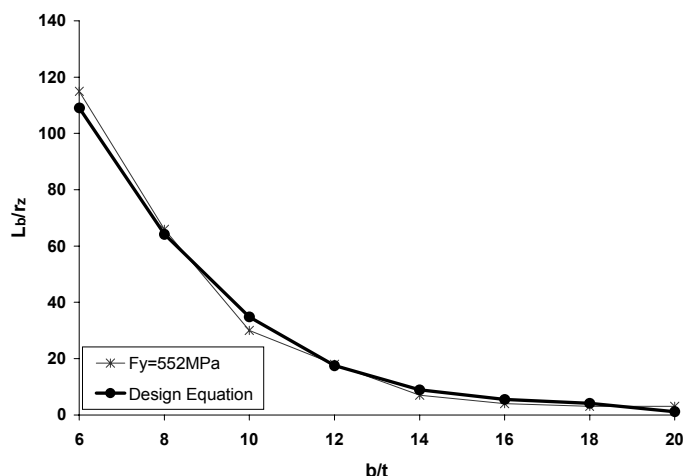
Fig. 13. Comparison of results between FEM and proposed Case 3 design equation.

the definition of compactness adopted in Case 4 is: the combination of plate slenderness, b/t, and beam slenderness, L_b/r_z, at a given steel strength, that results in the moment-rotation plateau exceeding the theoretical plastic capacity of the cross-section while maintaining a value for θ_3/θ_1 between 1.65 and 1.75. It is noted that in this definition of compactness it is necessary to consider both cross-sectional proportions and unbraced length when limiting the ratio θ_3/θ_1. As a result, the current criterion deviates philosophically from those compactness criteria used in the AISC LRFD (AISC, 1999) that de-couple local and global buckling influences and hence prescribe compactness limits in terms of cross-sectional proportions only.

The results from the finite element modeling associated with this case are summarized in Table 2. In addition, these data are presented in graphical form in Figure 16 by way of a plot of beam slenderness versus plate slenderness for five different mild carbon steel yield strengths (276 MPa, 345 MPa, 414 MPa, 483 MPa, and 552 MPa). The trends exhibited by this plot are studied and the results presented in the following section.

It appears that at a given plate slenderness value, b/t, as the yield strength of the mild steel increases, the beam slenderness must diminish in order to maintain compactness. For a given steel yield strength, the relationship between beam slenderness, L_b/r_z, and the plate slenderness, b/t, is a mostly nonlinear one. However, it can be observed in Figure 16 that in the range of plate slenderness from 16 to 20, all of the previously disparate response curves merge into one. In addition, this single curve has a very linear character in this b/t range of 16 to 20. As for the rest of the responses (b/t ranging from 6 to 16), based on curve fitting analyses in the range of yield strengths from 345 MPa to

552 MPa, the relationship between L_b/r_z and b/t appears to be quadratic; while for the case where the steel yield strength is 276 MPa, the same response is cubic. At this time it is still not clear what the significance of this difference is in terms of overall single angle beam behavior. No clearly discernable differences in modal manifestation and evolution could be identified between the quadratic and cubic cases.

It is pointed out that the Case 4 results reported are obtained from models that assume ideal restraint at the angle boundaries in terms of out-of-plane deflections, warping, and twisting. Normally field connection conditions do not qualify as being ideal and current design specifications (AISC, 1999) allow for the introduction of effective length factors for out-of-plane deflections, twisting, and warping (Galambos, 1968) in consideration of differing boundary conditions. As mentioned earlier however, the application of effective length factors is entirely reasonable for design provisions based on rational modifications of classical elastic solutions, the present work is in no way related to such an approach. In fact, after a careful examination of the inelastic modal manifestations associated with the flexural case reported in the current work, it is observed that some combinations of b/t and L_b/r_z result in mode shapes that display very localized buckling behavior well away from the boundary conditions, while other cases exhibit more of a global manifestation that would involve the beam boundary conditions more directly. Hence it is difficult to say precisely how to address issues related to effective length in the prescription of design provisions for this single angle flexural case. It may even be that such an approach is not valid in this instance since the influence of the precise
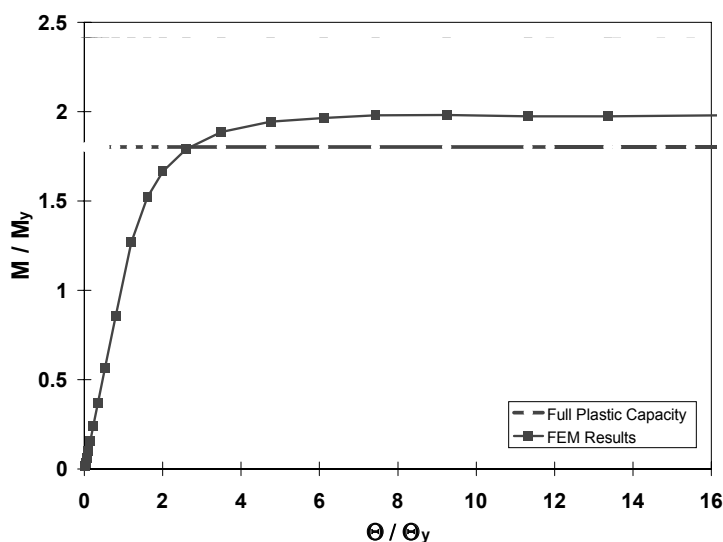

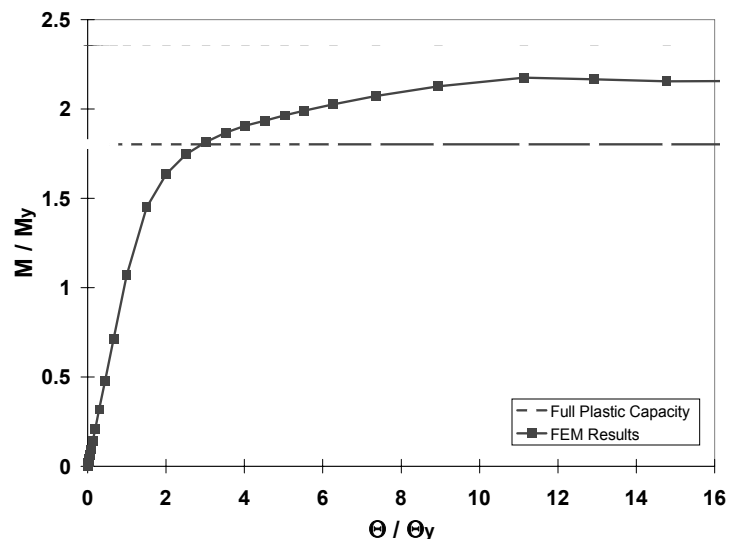Fig. 14.   Representative 345 MPa Case 4 moment-rotation response.

Fig. 15.   Representative Case 4 moment-rotation response for higher strength steel.

boundary conditions on the observed modal manifestation appears to vary on a case-by-case basis.

Throughout the process of analyzing the modeling results for the purposes of formulating a rational design procedure, simplicity is maintained as an important consideration. By virtue of this fact, a balance is struck between precise member response predictions and workable design provisions. The member response trends displayed in Figure 16 form the basis for the design methodology presented below.

In the proposed design approach a multi-linear fit to the individual L_b/r_z versus b/t responses is considered for each of the different mild carbon steel yield strengths. This approach is summarized by the following design equations developed as part of earlier research (Earls, 2001b):

For $10 \leq b/t \leq 20$ and 276 MPa $\leq F_y \leq 552$ MPa,

$$\frac{L_b}{r_z} = -1.9\left(\frac{b}{t}\right) + 39 \qquad (3)$$

and,
For $6 \leq b/t < 10$ and $F_y = 276$ MPa

$$\frac{L_b}{r_z} = -82.5\left(\frac{b}{t}\right) + 845 \qquad (4)$$

For $6 \leq b/t < 10$ and $F_y = 345$ MPa

$$\frac{L_b}{r_z} = -55\left(\frac{b}{t}\right) + 570 \qquad (5)$$

For $6 \leq b/t < 10$ and $F_y = 414$ MPa

$$\frac{L_b}{r_z} = -50\left(\frac{b}{t}\right) + 520 \qquad (6)$$

For $6 \leq b/t < 10$ and $F_y = 483$ MPa

$$\frac{L_b}{r_z} = -40\left(\frac{b}{t}\right) + 420 \qquad (7)$$

For $6 \leq b/t < 10$ and $F_y = 552$ MPa

$$\frac{L_b}{r_z} = -35\left(\frac{b}{t}\right) + 370 \qquad (8)$$

The proposed design compactness predictions contained in Equations 3 through 8 possess a certain degree of conservatism as can be seen qualitatively in Figure 17 which depicts the family of these design curves (Equations 3 through 8) plotted against the finite element results. This conservatism is most pronounced in the plate slenderness ranges of $b/t = 6$ and $10 \leq b/t < 12$ for the five yield strengths considered.
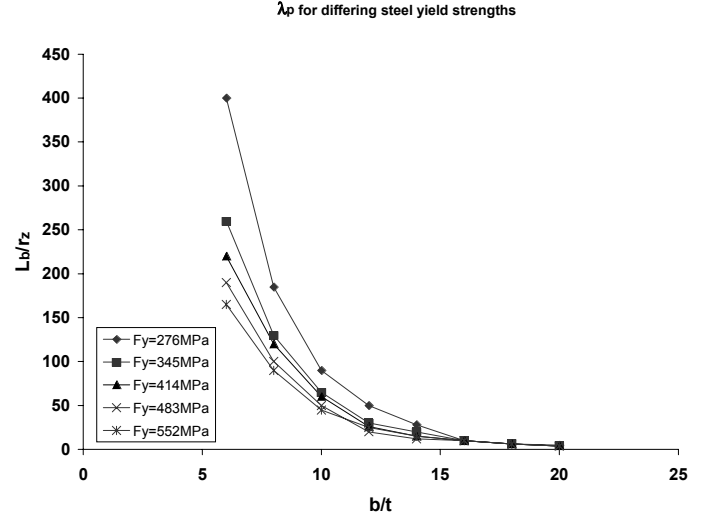

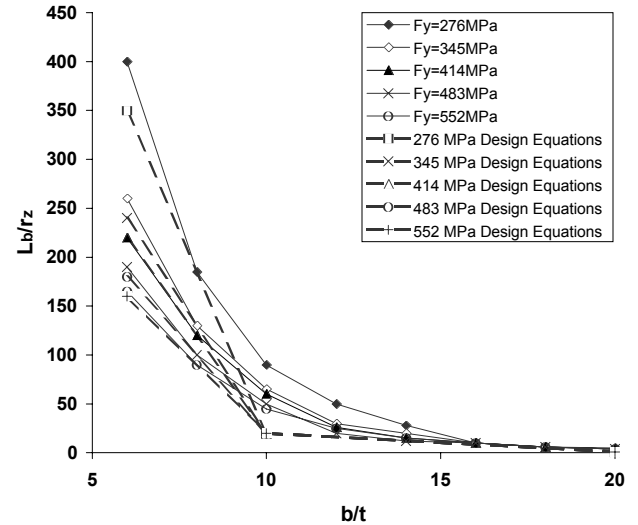Fig. 16.   Case 4 finite element compactness results.

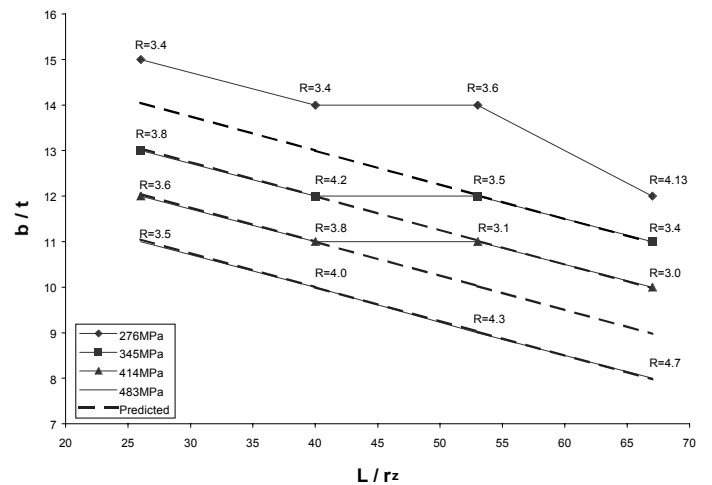Fig. 17.   Case 4 design method results.

Fig. 18.   Trends in major axis rotation capacity as affected by angle geometry and yield stress.

CASE 5. COMPACTNESS

Through the study of normalized moment-rotation curves resulting from finite element tests of single angles bent about the major principal axis it is possible to identify a minimum plate slenderness value associated with a given angle leg such that a rotation capacity of three is met or exceeded (Earls, 1999a). As with the other single angle flexural orientations, the unbraced length of the constant moment test segment plays an important role in affecting how ductile a single angle appears when subjected to major principal axis flexure. Hence it is essentially impossible to notionally de-couple localized buckling phenomena from more global manifestations of instability in the quantification of major principal axis single angle flexural ductility. This being the case, any specification of a Case 5 λ_p must include a dependence on the unbraced length of the flexural member. Based on earlier single angle research discussed above, it is expected that an increase in yield stress will result in a reduction in flexural ductility. Thus it is also necessary to consider the yield stress of the steel from which the angle is made in any prescription of λ_p. Tables 3, 4, 5, and 6 present a summary of compactness criteria obtained from this work.

It is interesting to note that despite the fact that all but three of the Case 5 cross-sections studied are classified as being slender by the *Specification* (meaning that the cross-sectional plate component will buckle at a stress lower than the yield stress), all of these specimens actually achieved or exceed the full plastic capacity of the cross-section while at the same time exhibiting a rotation capacity of three or more. This fact may support the argument that applying plate slenderness limits developed for columns (where the plate components are subjected to a uniform stress distribution) to the less critical case of angle beams (where a linear stress gradient is present) may be unduly conservative.

In the interest of identifying useful trends between the three parameters of yield strength, unbraced length, and plate slenderness, a family of curves is made with a plot of angle b/t versus beam slenderness L_b / r_z with the yield stress being changed incrementally. Figure 18 displays the results of such graphing. The solid lines correspond to the response at a given yield stress. It is observed that the curves of constant yield stress, while hinting at a linear trend, never quite justify such a simplification. Factors that directly bear on the shapes of the trend lines emanate from the choice to use integer values for the variation of the parameter b/t. This use of integer values results in a higher degree of scatter about the rotation capacity $R = 3$ (but always on the high side.) The angle cross section is considered to be compact if it exhibits a rotation capacity equal to or greater than three. Oftentimes a deviation in plate slenderness of one integer value results in a very significant increase in the observed rotation capacity. Thus a cross-section that barely fails to meet the $R = 3$ criterion may then

exhibit an R-value higher than 4 with a subsequent increase of one integer value in b/t. Similarly, the shape of the normalized moment-rotation responses themselves, contribute to the variability in the rotation capacity R. This is true due to the fact that the moment-rotation response flattens-out significantly as the compact section size is approached, thus slight changes in the shape of the moment-rotation curve results in quite a large change in the measured rotation capacity R.

In the interest of conservatism and simplicity, a non-dimensional design expression is formulated based on the worst-case behavior observed in the plots of Figure 18. This worst case corresponds to the 483 MPa yield stress case. A linear non-dimensional equation is fit through the data corresponding to this case. This linear equation allows for scaling to different yield stresses and has the form:

$$\frac{b}{t} = -0.075\left(\frac{L}{r_z}\right) - 2900\left(\frac{F_y}{E}\right) + 20 \qquad (9)$$

Equation 9 is subject to the limitation:
276 MPa $\leq F_y \leq$ 483 MPa

The conservatism of this equation can be verified by observing the dashed lines that are superimposed on the actual single angle response presented in Figure 18. These dashed lines correspond to the prediction for the single angle response resulting from the use of the above equation.

SHAPE FACTORS

Based on the research results summarized in the present paper, it has been observed that current restrictions on single angle cross-sectional capacity are unduly conservative. The current capacity limits amount to the imposition of an upper bound on the single angle shape factor (this upper limit is currently set at 1.5). While it is agreed that the shape factor limit of 1.5 is appropriate for Case 1, 2, and 5, equal leg single angle flexure, it is unduly conservative for Case 3 and 4, geometric axis flexure. Based on recent research (Earls, 2001a and 2001b) it is clear that a shape factor of 1.8 may be safely applied to these cases.

CONCLUSIONS

Based on the research results from the last several years, surveyed herein, it appears that improvements to the *Load and Resistance Factor Design of Single-Angle Members* (AISC, 2000) are possible. Compactness and bracing provisions have been outlined in the present work that will allow for the proportioning of single angle beams to be carried out with plastic analysis and design methodologies. Furthermore, several of the restrictions on single angle cross-sectional capacity, as prescribed by the *Load and Resistance Factor Design of Single-Angle Members,* should be lifted.

Table 3. Case 5 Finite Element Results for $L/r_z \approx 26$				
L/r_z	b/t	F_y (MPa)	R	M_{max}/M_y
26.1	15	276	3.4	1.5
26.4	13	345	3.8	1.5
26.5	12	414	3.6	1.5
26.7	11	483	3.5	1.5

Table 4. Case 5 Finite Element Results for $L/r_z \approx 40$				
L/r_z	b/t	F_y (MPa)	R	M_{max}/M_y
39.4	14	276	3.4	1.5
39.7	12	345	4.2	1.5
40	11	414	3.8	1.5
40	10	483	4.0	1.5

Table 5. Case 5 Finite Element Results for $L/r_z \approx 53$				
L/r_z	b/t	F_y (MPa)	R	M_{max}/M_y
52.4	14	276	3.6	1.5
53.0	12	345	3.5	1.5
53.3	11	414	3.1	1.5
54.3	9	483	4.3	1.5

Table 6. Case 5 Finite Element Results for $L/r_z \approx 67$				
L/r_z	b/t	F_y (MPa)	R	M_{max}/M_y
66.2	12	276	4.1	1.5
66.7	11	345	3.4	1.5
67.2	10	414	3.0	1.5
68.6	8	483	4.7	1.5

REFERENCES

ABAQUS (1999), *ABAQUS Theory Manual,* Hibbitt, Karlsson & Sorensen, Inc., Pawtucket, Rhode Island, USA.

ASCE (1971), *Plastic Design in Steel, A Guide and Commentary*, American Society of Civil Engineers, New York, New York, p. 80.

AISC (1999), *Load and Resistance Factor Design Specification for Structural Steel Buildings*, American Institute of Steel Construction, Inc., Chicago, Illinois.

AISC (2000), *Load and Resistance Factor Design of Single-Angle Members*, American Institute of Steel Construction, Inc., Chicago, Illinois.

Crisfield, M. A. (1981), "A Fast Incremental/Iterative Solution Procedure that Handles 'Snap-Through,'" *Computers & Structures*, Vol. 13, Pergamon Press Ltd., Great Britain, pp. 55-62.

Earls, C. J. (2001a), "Single Angle Geometric Axis Flexural Compactness Criteria: Horizontal Leg Tension," *Journal of Structural Engineering*, American Society of Civil Engineers, Reston, Virginia, Vol. 127, No. 6, pp. 616-624.

Earls, C. J. (2001b), "Geometric Axis Compactness Criteria for Equal Leg Angles: Horizontal Leg Compression," *Journal of Constructional Steel Research*, Elsevier Science Ltd., Great Britain, Vol. 57, pp. 351-373.

Earls, C. J. (2001c), "Single Angle Geometric Axis Flexure, Part I: Background and Model Verification," *Journal of Constructional Steel Research*, Elsevier Science Ltd., Great Britain, Vol. 57, pp. 603-622.

Earls, C. J. (2001d), "Single Angle Geometric Axis Flexure, Part II: Design Recommendations," *Journal of Constructional Steel Research*, Elsevier Science Ltd., Great Britain, Vol. 57, pp. 623-646.

Earls, C. J. (2000), "On Geometric Factors Influencing the Structural Ductility of Compact I-Shaped Beams," *Journal of Structural Engineering*, American Society of Civil Engineers, Reston, Virginia, Vol. 126, No. 7, pp. 780-789.

Earls, C. J. (1999a), "On Single Angle Major Axis Flexure," *Journal of Constructional Steel Research*, Elsevier Science Ltd., Great Britain, Vol. 51, No. 2, pp. 81-97.

Earls, C. J. (1999b), "Effects of Material Property Stratification on Single Angle Flexural Ductility," *Journal of Constructional Steel Research*, Elsevier Science Ltd., Great Britain, Vol. 51, No. 2, pp. 147-175.

Earls, C. J. (1999c), "On the Inelastic Failure of High Strength Steel I-Shaped Beams," *Journal of Constructional Steel Research*, Elsevier Science Ltd., Great Britain, Vol. 49, No. 1, January 1999, pp. 1-24.

Earls, C. J. and Galambos, T. V. (1998), "Practical Compactness and Bracing Provisions for the Design of Single Angle Beams," *Engineering Journal*, American Institute of Steel Construction, Inc., Vol. 35, No. 1, First Quarter 1998, pp. 19-25, Chicago, Illinois.

Earls, C. J. and Galambos, T. V. (1997a), "Design Recommendations for Single Angle Flexural Members," *Journal of Constructional Steel Research*, Elsevier Science Ltd., Great Britain, Vol. 43, Issue 1-3, July- September 1997, pp. 65-85.

Earls, C. J. and Galambos, T. V. (1997b), "Effects of Material Properties on Single Angle Compactness Requirements," *Proceedings of the Structural Stability Research Council Annual Technical Session*, Toronto, Canada.

Earls, C. J. (1995), "On the Use of Nonlinear Finite Element Analysis Techniques to Model Structural Steel Angle Response," *Ph.D. Dissertation*, University of Minnesota, Minneapolis, Minnesota.

Galambos, T. V. (1968), *Structural Members and Frames*, Prentice-Hall Inc., Englewood Cliffs, New Jersey, p.108.

Lay, M. G. and Galambos, T. V. (1965), "Experiments on High Strength Steel Members," *Welding Research Council Bulletin*, Bulletin No. 110, pp. 1-16, November.

Madugula, M. K. S., Kojima, T., Kajita, Y., and Ohama, M. (1995), "Minor Axis Bending Strength of Angle Beams," *Proceedings of the International Conference on Structural Stability and Design*, pp. 73-78, Sydney, Australia.

Madugula, M. K. S., Kojima, T., Kajita, Y., and Ohama, M. (1996), "Geometric Axis Bending Strength of Double-Angle Beams," *Journal of Constructional Steel Research*, Vol. 38, No. 1, pp. 23-40, Elsevier Science Ltd., Oxford, United Kingdom.

Madugula, M. K. S. and Kennedy, J. (1985), *Single and Compound Angle Members Structural Analysis and Design*, Elsevier Applied Science Publishers, New York, New York.

Riks, E. (1972), "The Application of Newton's Method to the Problem of Elastic Stability," *Journal of Applied Mechanics*, Vol. 39, American Society of Mechanical Engineers, pp. 1060-1066.

Riks, E. (1979), "An Incremental Approach to the Solution of Snapping and Buckling Problems," *International Journal of Solids and Structures*, vol. 15, Pergamon Press Ltd., Great Britain, pp. 529-551.

Teh, L.H. and Clarke, M. J. (1999), "Tracing Secondary Equilibrium Paths of Elastic Framed Structures," *Journal of Engineering Mechanics*, Vol. 125, No. 12, American Society of Civil Engineers, Reston Virginia, pp. 1358-1364.

Thomas, B. F. and Leigh, J. M. (1970), "The Behaviour of Laterally Unsupported Angles," *Report MRL 22/4* December 1970, Melbourne Research Laboratories, Clayton, Australia.

Thomas, B. F. and Leigh, J. M. (1973), "The Behaviour of Laterally Unsupported Angles," *Civil Engineering Transactions*, The Institution of Engineers, Australia, pp.103-110.

Usami, T. and Galambos, T. V. (1971), "Eccentrically Loaded Single Angle Columns," *Proceedings of the International Association for Bridge and Structural Engineering*, Zurich, Switzerland.